Physics of Fluids

Spray droplet size distribution and droplet velocity measurements in a firing optical engine

Cite as: Phys. Fluids **32**, 023304 (2020); https://doi.org/10.1063/1.5126498
Submitted: 03 September 2019 • Accepted: 02 December 2019 • Published Online: 04 February 2020

Nikhil Sharma, William D. Bachalo and Avinash Kumar Agarwal

AIP Publishing

Spray droplet size distribution and droplet velocity measurements in a firing optical engine

Cite as: Phys. Fluids 32, 023304 (2020); doi: 10.1063/1.5126498
Submitted: 3 September 2019 • Accepted: 2 December 2019 •
Published Online: 4 February 2020

Nikhil Sharma,[1] William D. Bachalo,[2] and Avinash Kumar Agarwal[1,a)]

AFFILIATIONS

[1] Engine Research Laboratory, Department of Mechanical Engineering, Indian Institute of Technology Kanpur, Kanpur 208016, India
[2] Artium Technologies, Inc., Sunnyvale, California 94085, USA

[a)] Author to whom correspondence should be addressed: akag@iitk.ac.in

ABSTRACT

Macroscopic spray characteristics of a fuel injection system in an internal combustion (IC) engine have a direct impact on engine performance, emissions, and combustion characteristics. Nonintrusive in-cylinder measurements provide insights into the spray formation process for greater understanding of fuel-air mixing and combustion processes in an IC engine. In this paper, there are two parts: (a) procedure and methodology to configure the Artium phase Doppler interferometer (PDI) for *in situ* measurements through a cylindrical window and (b) comparative macroscopic spray characteristics in a firing Gasoline Direct Injection (GDI) optical engine to a constant volume spray chamber (CVSC) for spray droplet size-velocity distributions. Binned average velocity and average Sauter mean diameter of spray droplets in a firing engine were compared with that of a CVSC. Probability density function of droplet diameters in the CVSC under ambient conditions and in the engine combustion chamber provides an insight into the comparative droplet size distributions and droplet dynamics. Discussion on challenges encountered during PDI measurements in the firing engine environment, safety protocols, and tools required is also included. In addition, shadowgraphy images have been used to discuss the details on spray boundaries and spray evolution. The droplet size distribution inside the engine combustion chamber was found to be significantly different from the one observed in the CVSC. An engine simulation model can be developed/validated by using the data reported in this manuscript for attaining superior accuracy in the model. This paper describes the comparisons of the spray droplet size and velocity distributions in a CVSC and *in situ* for a working GDI engine. Maximum spray droplet velocity components (V_x, V_y) under engine combustion chamber conditions were 29.8 m/s, 14.2 m/s whereas the corresponding velocities in the CVSC under ambient conditions they were 78.41 m/s, 23.92 m/s, respectively, showing a large difference between the traditional measurements in the CVSC simulating engine conditions, and actual firing engine conditions. This study also reports the very first attempt in the open literature to measure spray droplet size and velocity distribution measurements in a firing IC engine.

I. INTRODUCTION

Accurate size and velocity measurements of liquid sprays are important for a broad range of applications.[1,2] Gasoline Direct Injection (GDI) engines have undergone exceptional improvements and refinement in last couple of decades to be able to deliver fuel at high fuel injection pressure (FIP) with an objective of achieving enhanced fuel efficiency and improved power output.[1,3] Higher FIP leads to better fuel atomization and, consequently, superior fuel-air mixing. High pressure fuel injection, as in the case of GDI engine sprays, adds complexity in measurements of the droplet size and velocity distributions, especially inside an engine combustion chamber.[4] This is primarily because the GDI spray plumes are closely spaced and, hence, are likely to interact, merge, or eventually collapse. This interaction also complicates the droplet evaporation, atomization, collision, breakup, coalescence, and energy exchange processes among GDI spray droplets. A numerical investigation of binary droplet collision has been conducted by Pan and Suga[5] and is of interest in volume-limited applications such as internal combustion (IC) engines. The authors reported the feasibility of applying the level set method to liquid/gas systems with high density ratios above 500, which is typical in many practical applications such as gasoline or diesel injection into air. In a GDI engine, sprays with small droplets but high fuel flow rates over short durations are required for fuel induction into the engine combustion chamber. Due to these complexities, investigating fuel sprays and fuel-air mixture formation processes in the GDI engine combustion chamber remains critical because fuel-air mixture quality eventually affects engine performance, emissions, and combustion characteristics.[6,7] Higher FIP leads to smaller spray droplets, thus increasing the droplet surface area, which comes in direct contact with the surrounding air, improving their evaporation, and thus improving the fuel-air mixing.[8] However, flow in the IC engine depends on the engine type and operating condition, which affects the spray droplet size distribution.[9]

Spray atomization also depends on the pressure difference between the in-cylinder pressure and the FIP, which also dictates the spray droplet velocity. The superior fuel-air mixture formation, therefore, not only depends on the droplet size distribution, but also on the spatial distribution and dynamics of spray droplets in the engine combustion chamber environment. There is a vast volume of literature available on spray atomization,[10] which can be broadly divided into two parts. The first type of spray droplet atomization investigation is related to the stability of fuel spray jet, ligament formation, macroscopic spray characteristics, and spray breakup.[5,11,12] However, most such studies involve numerical simulations and they provide mathematical expressions such as average, maximum, or minimum values of different spray droplet parameters. The second type of spray droplet atomization investigation deals with the spray droplet size distribution, droplet velocity distribution, and parameters such as Sauter mean diameter (SMD) of the sprays with specific physical interpretation.[13,14]

Liquid fuel atomization studies and spray droplet size distribution measurement techniques are explicitly described in open literature.[15–17] In these papers, spray droplet distribution measurement methods are classified into three main categories: (a) mechanical, (b) electrical, and (c) optical spray measurement methods. Vukasinovic *et al.*[18] performed vibration-induced droplet atomization resulting in smaller droplets from larger droplets, which were further characterized using high-speed imaging and particle-tracking techniques. However, today, most researchers use nonintrusive spray diagnostics techniques such as Schlieren, shadowgraphy, Mie and Rayleigh scattering, diffuse backlit illumination (DBI), particle imaging velocimetry (PIV), laser absorption, scattering, Raman spectroscopy, laser induced fluorescence (LIF), phase Doppler interferometry (PDI)/phase Doppler anemometry (PDA), etc., for these investigations. PDI or PDA techniques were developed by Bachalo[1,19] in the 1980s to measure the spray droplet size and velocity distributions simultaneously. Following these initial innovations, PDI has evolved and matured as an established point measurement technique for the spray droplet size and velocity distribution as well as volume flux measurements at high frequency up to tens of thousands hertz.[20,21] In addition, the ability to confine measurements to smaller particles allowed the measurement of gas phase turbulence in the presence of a dispersed phase such as in a fuel spray combustion. The spray measurement studies were of great interest to gas turbine and diesel engine community. Subsequently, GDI sprays have also emerged as an area of research interest for engine developers, in a quest to develop more efficient and cleaner burning engines. Numerous studies have been conducted by researchers on GDI spray characterization. Yamakawa *et al.*[22] emphasized on the internal structure of liquid jets, spray atomization processes, and fuel evaporation characteristics. These were the three critical factors responsible for fuel-air mixture quality, which eventually affect combustion and pollutant formation. Lee and Park[23] investigated the effect of FIP on droplet size distribution of a spray generated by a six-hole GDI injector at different FIPs (5, 10, 20, and 30 MPa). They reported that the maximum droplet diameter decreased from 13.11 μm to 9.45 μm, when FIP increased from 5 MPa to 20 MPa. With further increase in the FIP to 30 MPa, reduction in the maximum droplet diameter was insignificant, though. In a similar study, Lee and Park[23] measured SMD (ensemble average of spray droplet diameter distribution) 50 mm downstream of the injector nozzle at different FIPs. They reported that SMD decreased linearly when FIP was increased from 5 to 20 MPa. Beyond 20 MPa, no significant reduction in SMD was observed. Thus, it was concluded that although increased FIP enhances spray atomization, there exists a limiting value, beyond which FIP does not play a significant role in improving the spray atomization. Injectors with multiple holes can be more effective in reducing the droplet sizes (reduced SMD) compared to a single-hole Injector.[23] Fuel properties also have a significant impact on spray droplet size distribution. Park *et al.*[24] reported that due to higher kinematic viscosity and surface tension of gasoline than other test fuels (E100 and E85), gasoline exhibited larger droplet size distributions. However, Anand *et al.*[25] reported nearly similar droplet size distribution but significantly different spray droplet velocity distribution, while investigating spray characteristics of different fuels such as gasoline, ethanol, and gasoline-ethanol blends containing 10%, 20%, and 50% ethanol for sprays emerging from a 4-hole port fuel injected (PFI) injector. Heldmann *et al.*[26] performed experiments in a spray chamber to explore spray atomization and evaporation of gasoline, ethanol, and butanol using phase Doppler anemometry (PDA, aka PDI). They reported that relatively higher viscosity of ethanol and butanol decreased the Reynolds number, which in-turn reduced spray atomization. However, the situation could be improved by increasing the test fuel temperature. Similar observations related to increased fuel temperature were also reported by Huang *et al.*[27] The PDA technique was also employed by Aleiferis *et al.*[28] to measure the spray droplet size distribution in the core of one of the spray plumes, 25 mm downstream of the injector tip for E85 and gasoline. They reported that in-nozzle cavitation was more severe for gasoline, which resulted in smaller droplet size distribution compared to E85. Sharma and Agarwal[29] investigated spray droplet size-number distributions under ambient conditions for different renewable fuels. They reported that the spray droplets generated at lower FIP were less scattered and as the FIP increased, the droplets dispersed more in different directions. Agarwal *et al.*[30] performed an experimental study to investigate effects of intake port geometries on air-flow characteristics using tomographic particle imaging velocimetry (TPIV). Authors reported that in the compression stroke, the highest vorticity zones were in the vicinity of the cylinder head. However, no results pertaining to droplet size/velocity distribution were reported. Investigations on the breakup and coalescence characteristics of a hollow cone swirling spray were performed by another researcher, which utilized only phase Doppler interferometry and shadowgraphy techniques to quantify the velocity, droplet shapes, and diameter distributions.[31] Most of these studies were conducted in spray chamber under different ambient chamber pressure/temperature conditions (cold/nonreacting environments), which are not truly reflective of the environment faced by fuel spray under realistic engine conditions. To overcome this, many assumptions are made in numerical or simulation studies to understand the spray evolution process, such as uniform air flow field, no fuel evaporation, no drag on spray droplets, numerical stability, and degree of convergence of results.[32] In order to understand these important and fundamental phenomenons governing engine combustion, efficiency, and pollutant formation, it is important to conduct experimental investigations for GDI spray characterization in a firing engine, so that real time information about the spray evolution in an engine combustion chamber environment can be extracted.

In this paper, the PDI instrument has been used for spray characterization in an optical GDI engine to understand the spray evolution in terms of the droplet size and velocity distributions. Challenges faced, step-by-step procedure adopted for making these measurements, and methodology followed to align the laser beams of the phase Doppler interferometer (PDI) instrument before attempting to perform GDI spray evolution measurements through a cylindrical optical window are discussed at length. Discussion on challenges encountered during PDI measurements, safety of personnel, and tools required for making such challenging measurements have also been provided. Thereafter, a comparative analysis of the droplet size and velocity distributions inside an optical GDI engine combustion chamber and inside a constant volume spray chamber (CVSC) under ambient conditions is also performed. The droplet size distributions inside the engine combustion chamber were found to be significantly different from that observed in the CVSC. Apart from this, shadowgraphy of the spray plumes has been used to discuss minute details of the spray boundaries. The present experimental investigation of spray droplet size distribution and dynamics within a firing IC engine is unique and, the droplet-size distribution data in a firing optical engine are not reported in the literature before. This pioneering work will be important for improvements in combustion efficiency and for improving the design of engines. This study includes spray droplet sizing information from an engine environment, which will be extremely helpful to engine designers and simulation engineers.

II. APPROACH

i. Design and construct a CVSC rig for spray characterization using PDI.
ii. Perform microscopic spray experiments in the CVSC under ambient chamber pressure conditions.
iii. Develop a methodology for laser beam alignment using highly polished mirrors to redirect the laser beams and for collecting scattered light to allow *in situ* measurements of the droplet size and velocity distributions in the optical engine's combustion chamber. This methodology involved the alignment of optics outside the optical engine by using a surrogate optical window and a 3D traverse.
iv. Setup PDI and 3D traverse in the optical engine test rig and align the laser beams using methodology developed using surrogate window in step (iii).
v. Compare the results of the droplet size and velocity distributions from the CVSC to the real firing GDI engine conditions.

III. MEASUREMENT ENVIRONMENT CHALLENGES

A two-component PDI instrument is a temperature sensitive instrument, wherein two solid-state lasers are packed in a single transmitter. These lasers must be maintained within a certain temperature range in order to avoid any changes in laser beam intensity and to avoid laser power pulsations. For engine measurements using PDI, the engine control room can be air-conditioned and maintained in a suitable temperature range. However, engine test cells may generally not be air-conditioned. Therefore, it becomes difficult to perform PDI engine experiments during summer, when the test cell temperatures may rise above 40 °C. Another major challenge is the limited engine operating window for the optical engine, which cannot exceed approximately 30 s due to unacceptable increase in the optical cylinder temperature. If the engine is fired for periods longer than 30 s in one step, high in-cylinder temperature will damage the optical window, leading to its catastrophic failure due to excessive thermal expansion of the optical components. Optical access to the engine combustion chamber via the optical liner is often made more difficult by the surrounding spray droplets that attenuate, scatter and deflect the incoming laser beam.[10] This can lead to spurious and noisy signals. It requires frequent cleaning of the cylindrical optical window after every measurement of less than 30 s, which makes engine measurements a time-consuming and challenging task. Depending on the engine design, the engine cylinder head is required to be disassembled to enable the cylindrical optical liner removal for cleaning, followed by reassembly of the engine for the next set of measurements. There are a few fittings, structural members, and accessories, which are essential to operate the engine, but they create obstructions of the laser beam path, making the measurements challenging. The laser beams need to be oriented at a specified angle, so that they intersect at the measurement point located inside the engine combustion chamber, right below the fuel injector at a location, where the measurements need to be taken. The beams must also be at a specific angle to the receiver, typically at 30° from the projected beams.[19] 30° provides a very good separation between the light scattered by refraction (desired mechanism) and reflection and diffraction (undesired). In addition, the light scattering intensity decreases with the increasing light scattering angle. Therefore, detection at 30° provides an optimum condition in terms of the signal to noise ratio and separation of the undesired light scattering mechanisms. An additional advantage of using 30° light scattering is that the optical access to the engine allows a larger range of traversing distances of the measurement volume to better cover the spray plume. This challenging problem of limited optical access may be resolved by using highly polished mirrors, which can be used to reflect the laser beams to avoid the obstacles. However, it is likely that the second transmitter (used for measurement of the third component of velocity, having one laser) may not be used due to the limited space in the optical window for the measurements. It is quite likely that out of the 4 laser beams emerging from the first transmitter, one or more laser beams may be blocked by the engine's structural pillars. This may limit the formation of the probe volume at different locations inside the engine combustion chamber, thus limiting the choice of measurement points. PDI instruments may be sensitive to electrical noise in the working environment. Noise emanating from many sources used in an engine test cell environment can create signal to noise issues. Therefore, a good common grounding should be included in the test cell. Fortunately, the PDI uses advanced digital signal detection means and validation criteria that minimize the adverse effects of electronic noise. Quantification of the associated uncertainties and validation criteria is given in the supplementary material. Based on these observations, it is amply clear that numerous challenges and difficulties exist in making detailed spray measurements in an engine using PDI, and there is a risk of either not getting the results or getting biased results due to such operational difficulties. However, even in the presence of these constraints, it is possible to perform accurate spray measurements.

IV. LASER BEAM ALIGNMENT AND MEASUREMENT CHALLENGES DUE TO REFRACTION AND REFLECTION FROM OPTICAL WINDOW

Before aligning the laser beam in the optical engine, it is important to understand the reflection and refraction of lasers through two different media. For the current setup, two blue laser beams traverse in a horizontal plane, whereas two green laser beams traverse in the vertical plane [Figs. 1(a) and 1(c), when the cylinder axis is vertical] for measurement of droplet velocity components and size distributions.

Reflection and refraction of laser beam through two different media having different refractive index, n_a and n_b, are shown in Fig. 1(b). When light travels from one medium to another, part of the light (approximately 15%) is reflected from the interface of the two materials, while most of the light enters the second medium. Reflection is therefore defined as a phenomenon, in which light is reflected into the same medium after it strikes the interface of the two media. On the other hand, refraction involves change in the direction of the light passing from one medium to another, caused by its change in speed. More details about diffraction, reflection, and refraction from spherical objects such as fuel spray droplets are available in open literature.[33]

Laser beam alignment is very sensitive to the quality of optical windows as well as to the quality of laser beam. Thickness, optical window quality, curvature, and laser beam quality may contribute to errors in measurements. For a two-component system, one pair of laser beams in a plane is parallel to the optical window axis, while the other pair is perpendicular to the optical window axis. The pair of beams in a plane perpendicular to the cylinder axis enters orthogonal to the cylinder surface when they are aligned to cross at the centerline of the cylinder. The direction of these beams is not affected significantly by the cylindrical surface. The beams in a plane parallel to the cylinder axis will be deflected due to their angle of incidence to the optical window. This will change the location of the intersection point of that pair of beams. During alignment of the laser beams for spray measurements, refraction of the laser beam must be considered. If the measurement point is at the center of the cylindrical optical window, alignment of the laser beam becomes easier because one of the lasers beams (blue: horizontal plane traversing) will not refract and will remain at the center. However, if the measurement point is away from the center of the cylindrical optical window, then both beams will refract slightly from their normal path. The laser beams refract according to Snell's Law, which is given as

$$m_1 \sin \gamma_1 = m_2 \sin \gamma_2 \qquad (1)$$

where m_1 and m_2 are the refraction indices of the two media, through which the beam is traversing (m = 1 for air and m = 1.5 for glass), and γ_1 and γ_2 are the angles that the beam makes with the normal to the surface. The term "alignment of laser beams" means that all laser beams (four in number, 2 blue and 2 green) must intersect at a single point, which is called the "probe volume," the location where spray measurements would be performed. However, due to refraction, laser beams (green) may deviate a little from the actual positions. Therefore, the adjustment of beams is required such that they intersect at the desired measurement point. It is difficult to perform such alignment without a surrogate optical window placed on the 3D traverse outside the engine. The approach is to align the beams to a specific point in the surrogate optical cylinder to ensure that all four beams are intersecting at the same location and that location is known based on the traversing system location. The instrument is then traversed to the same location within the engine. For each subsequent measurement point within the cylinder, the beams must be realigned to that location before moving to the engine and the same location inside the engine cylinder. The process is painstaking but necessary to ensure high quality drop size and 2D velocity measurements. More details on dealing with small droplet measurements and dense sprays may be found in Sankar *et al.*[34] A detailed alignment procedure of laser beams for optical engine and safety instructions while dealing with alignment is given in supplementary material.

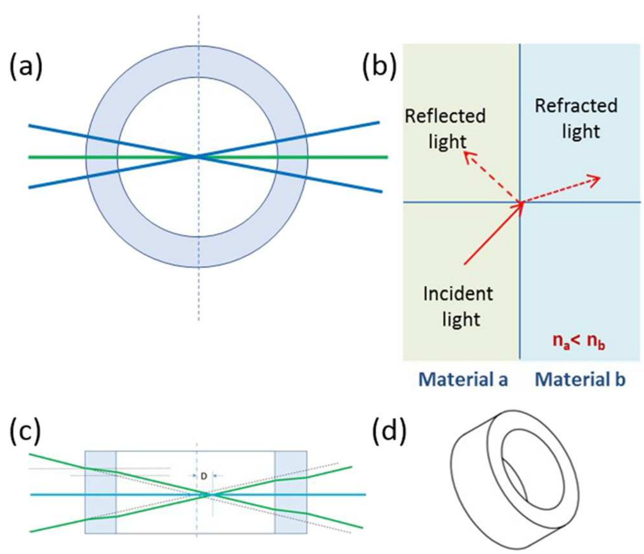

FIG. 1. Refraction and reflection of laser light beams in a cylindrical optical window of the engine combustion chamber. (a) Top view of the optical cylinder window showing laser beam propagation, (b) refraction and reflection of laser light beams by the optical window, (c) side view of the optical cylinder window showing laser propagation, and (d) optical window geometry.

V. EXPERIMENTAL SETUP AND METHODOLOGY

The experiments in this study are done under ambient chamber pressure conditions in a CVSC and under identical atomization conditions in an actual firing engine environment for comparative analyses. Two experimental setups (i) CVSC and (ii) GDI engine were therefore used and PDI experiments were performed in both facilities.

The CVSC experimental setup was developed to understand the behavior of fuel sprays in a cold nonreacting high-pressure environment. The CVSC consisted of seven flanges, out of which

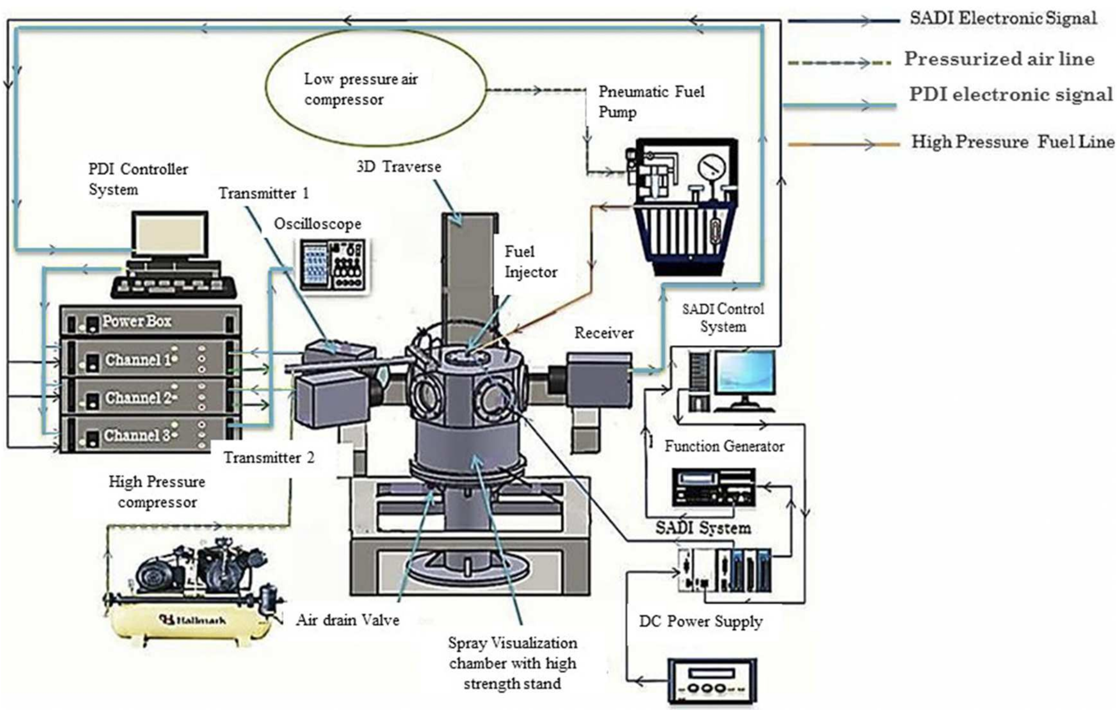

FIG. 2. Schematic of CVSC for microscopic spray measurements.

five flanges had quartz windows and the remaining two have metallic windows. One of the metal flanges was located on the top of CVSC to hold the injector and the other metal flange at the bottom supported the drain valve for continuous air purge from the CVSC. This CVSC experimental setup (Fig. 2) for microscopic spray analysis consists of (i) fuel injection system, (ii) CVSC with air purging system, and (iii) PDI system. Each of these subsystems consists of several components and devices.

The Artium 3D PDI system consisted of two transmitters, one receiver, three signal analyzers and a computer. Technical specifications of PDI are given in Table I. Two transmitters delivered six laser beams, which intersected at a point called to form the probe volume. The PDI instrument measures the droplet size and velocity simultaneously with one channel measuring the drop size and one component of the velocity. A second pair of laser beams disposed orthogonal to the first pair is used to measure the orthogonal velocity component. Hence, the droplet size and two components of droplet velocity are measured simultaneously. The diameter is measured for every droplet. The diameter measured is orthogonal to the plane of the respective laser beams performing the measurements.

For this experiment, four laser beams (green and blue) were made to converge at a single point inside the CVSC from one

TABLE I. Technical specifications of PDI.

Technical Specifications of PDI	
Droplet size measurement range	0.3 to >2000 μm (spherical or near-spherical particles)
Size dynamic range	50–1 dynamic range selectable by the software (e.g., 1–50, 2–100, etc.)
Estimated size accuracy	±1 μm or 1% of full-size range
Estimated size resolution	±1 μm or 0.5% of full-size range
Velocity measurement range	−600 to 500 m/s
Velocity accuracy	±0.2%
Volume flux accuracy	±10%
Available receiver focal lengths	350 mm, 500 mm, 750 mm, 1000 mm
Available transmitter focal lengths	350 mm, 500 mm, 750 mm, 1000 mm
Laser type	Diode pumped solid state (DPSS)
Wavelength	491 nm, 532 nm, 561 nm

of the quartz windows, and the signal was captured by the PDI receiver from the other quartz window. The receiver was aligned with the transmitters in such a way that the angle between the receiver and the transmitter was maintained to be 30°. The transmitters and the receiver, both are mounted on a 3D traverse for the mobility of probe volume without affecting the laser beam alignment. A high-speed camera (Photron, SA 1.1) was used to visualize the spray evolution. The minimum frame rate for this camera is 5400 fps at maximum resolution and 675 000 fps at minimum resolution with a shutter exposure time from 16.7 ms to 1 μs.

Experiments were then performed on a single cylinder GDI, optical research engine (Mobiltech; HMC Seta 0.5L), which delivers a rated torque of 30 Nm @ 2000 rpm (Fig. 3). Specifications of the test engine are given in Table II and important properties of test fuels are given in Table III.

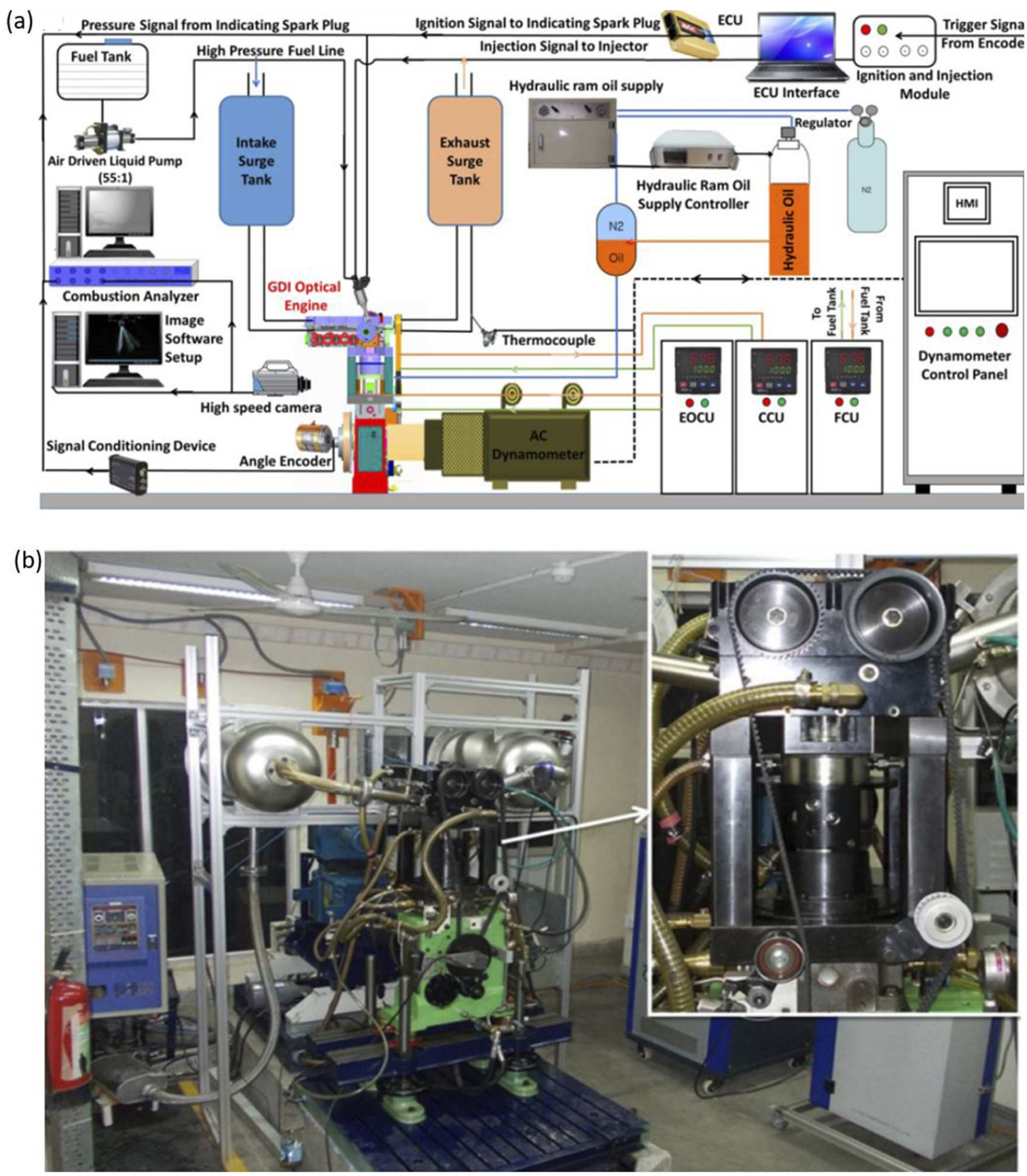

FIG. 3. (a) Schematic and (b) image of the GDI optical engine experimental setup for spray characterization.

TABLE II. Optical test engine specifications.

Engine type	Single cylinder GDI
Bore × Stroke	86 mm × 86 mm
Displacement	500 cc
Connecting rod length	196 mm
Compression ratio	10.5:1
Maximum power	6.28 kW @ 2000 rpm
Maximum torque	30 Nm @ 2000 rpm
No. of injector holes	6

Figure 3 shows the schematic and the image of experimental setup for the GDI optical engine. The optical engine consists of a hydraulic lock assembly unit, which facilitates quicker dismantling of the optical window for cleaning, without having to disassemble the cylinder head. The test engine was coupled with a 36-kW transient AC dynamometer (Dynomerk Controls; 6-2013). A precision optical shaft encoder (AVL; 365C) was mounted on the engine crankshaft, which delivered 720 pulses per revolution of the crankshaft. This encoder was attached to a 4-channel high speed combustion data acquisition and analysis system (AVL; Indimicro). The in-cylinder pressure signals from the indicating spark plug pressure transducer (AVL; ZI31_Y5S) were provided to the high-speed combustion data acquisition and analysis system, via a built-in charge amplifier. Intake air was maintained at 20 °C during the experiments. An ECU (MOTEC; m400) was a part of the test cell, which controlled the fuel injection timing, spark timing, and injector pulse width. The GDI injector peak and hold driver (Zenobalti; ZB-5100G) were also mounted on to the engine and were controlled by the open ECU. Piezoelectric injectors were used because they enable quick and accurate control of the injector needle's movement. These injectors open and close the needle using the pressure difference between the fuel injection and return flow.

Figure 4 shows the schematic and image of experimental setup for PDI spray characterization in GDI optical engine. The PDI system (Artium; PDI-300 MD) performs real-time, simultaneous non-intrusive measurement of droplet size distribution, and distribution of 2-velocity components of the spray droplets. The instrument consists of a two-component optical transmitter generating four intersecting laser beams, an optical receiver, advanced signal analyzers (ASA), a computer, and an automated instrumentation management system (AIMS) software for signal processing. High-power diode pumped solid state (DPSS) lasers used in the PDI transmitters were Class-3B lasers. Two laser beams, green (532 nm) with an intensity of 500 mW and blue (491 nm) with an intensity of 200 mW, emerged from the transmitter. The transmitter consisted of two Bragg cells for splitting the laser beam into two equal intensity beams and for frequency shift of one of the two laser beams. These four beams were then carefully aligned to merge at a single point with the help of a pin hole (~100 μm or less) with the point of merger of four laser beams forming the probe volume. The scattered light at the probe volume was then focused by the receiver lens system onto the detection aperture in the receiver package. This enabled collection of scattered light signals from the droplet/s passing through the probe volume. The optical receiver consisted of a lens and four photo detectors; three for the phase Doppler method on channel one to measure the drop size and velocity and one to measure the second velocity component. The scattered light for each wavelength is separated using optical filters. More details about the principle of measurement are given in the open literature.[10] For this experiment, a 500 mm focal length lens for the transmitter and a 350 mm focal length lens for the receiver were used. The selection of optical components is determined by the drop size ranges to be measured, the required size of the sample volume to avoid coincidence, and the ability to provide maximum size resolution. The optical access and size of the measurement environment also dictate the respective focal lengths of optical components. For example, with the engine measurements, the focal lengths were determined, in part, by the available space and access to the engine. In general, shorter focal length lenses on the transmitter produce a smaller probe volume diameter and higher resolution and accuracy for measuring small drops. Longer focal length lenses produce a larger probe volume and lower sensitivity to the smaller droplets in the size distribution. A wide range of optical combinations allows the measurement of droplets in the size range of 0.5–1000 μm. This study includes two sets of experiments: (a) Optical engine droplet size-velocity distribution and (b) Constant volume spray chamber (CVSC) droplet size-velocity distribution. For CVSC, the 500 mm focal length lens for the transmitter and 350 mm focal length lens for the receiver lenses were used. For engine experiments, 500 mm focal length lenses were used for the transmitter and the receiver. In engine experiments, the space constraints and engine peripheries such as cooling and lubricating pipes make it mandatory to use larger focal length lens. It was difficult to form a probe volume at the intersection of laser beams with 500 mm focal length lens, due to space limitation, therefore, two highly polished adjustable mirrors, one for the transmitter and the other one for the receiver, were used to reflect the laser beams and the scattered light signal in a specified space and it allowed the placement of transmitter and receiver slightly away from the hot and vibrating engine cylinder as shown in Fig. 4. In addition, a high-speed camera was used for shadowgraphy of the spray.

TABLE III. Important test fuel properties.

Fuel	Gasoline
Molecular formula	C_4–C_{12}
Density @ 20 °C	0.745 g/cm^3
Kinematic viscosity	0.494 mm^2/s @ 40 °C
Oxygen content	< 0.05% w/w
Research octane number	95
Stoichiometric air/fuel ratio	14.7
Surface tension	18.93×10^{-3} N/m @ 27 °C

VI. RESULTS AND DISCUSSION

In this section, a comparative analysis of the microscopic spray characteristics such as spray droplet velocity and mean droplet size distribution between CVSC and real time engine conditions are described. The methodology/protocol described in the

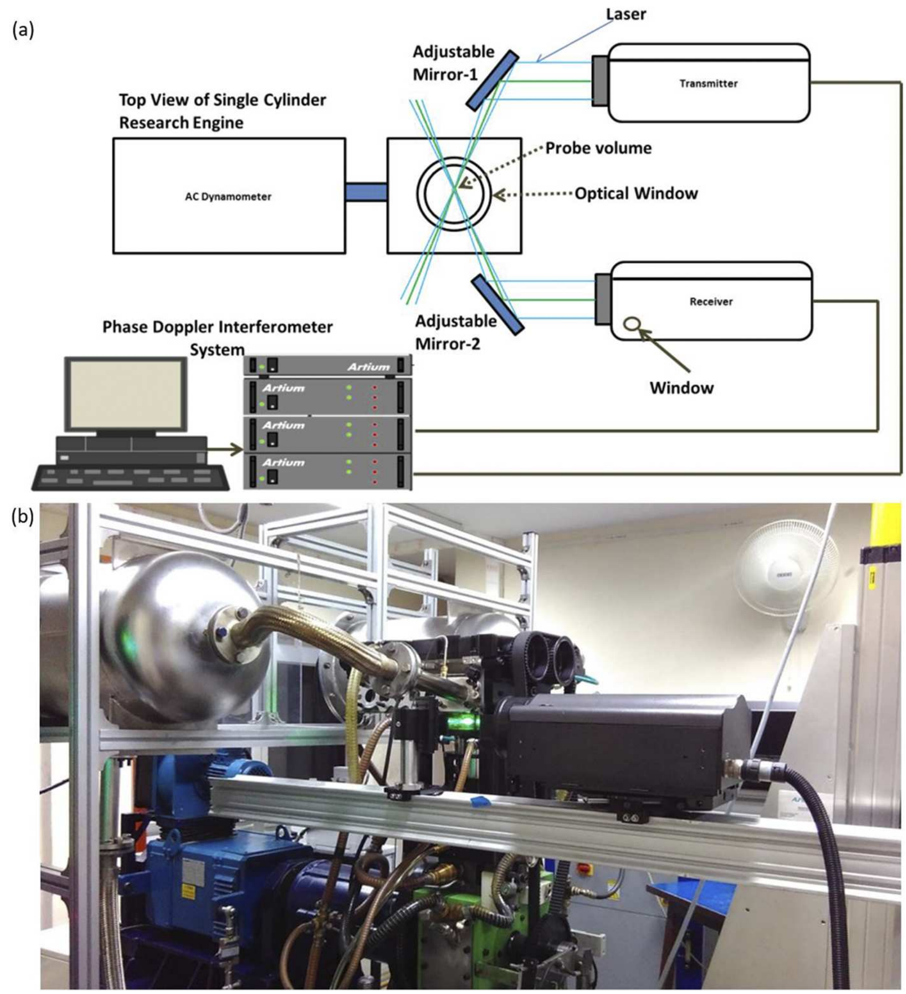

FIG. 4. (a) Schematic and (b) image of experimental setup for PDI spray characterization in GDI optical engine.

open literature by Bachalo has been adapted in this experimental study.[10]

The major forces for droplets include the drag force ($\overrightarrow{F_D}$), which results from the velocity difference between the gas and the liquid phases, and the gravitational and buoyancy force ($\overrightarrow{F_g}$). The basic equation for droplet motion is therefore given as

$$\sum F = (\overrightarrow{F_D}) + (\overrightarrow{F_g}) = m_p \frac{d_{u_{p,i}}}{dt}, \tag{2}$$

where m_p is the mass of droplet and $u_{p,i}$ is the velocity of the droplet in the direction "i."[35]

The fuel-air mixture in the combustion chamber is affected by the fuel properties (such as fuel density, viscosity, and surface tension) as well as the mixing rate of fuel and air. The GDI injector performs three important functions: liquid fuel atomization, fuel distribution in the combustion chamber air, and consequent fuel-air mixing. For the sake of simplicity, the phenomenon is explained using a single droplet in the engine combustion chamber. Figure 5 shows the schematic of a piston cylinder arrangement, with a single fuel droplet considered for easier explanation of the processes taking place in a firing engine. As the piston moves from top dead center (TDC) to the bottom dead center (BDC), fuel is injected, and the fuel droplets experience drag from all sides in a high-temperature and high-pressure environment. Each droplet experiences the high intensity large- and small-scale turbulence inside the engine combustion chamber, before it evaporates and finally gets ignites by the spark ignition. The difference between the in-cylinder pressure and FIP dictates the fuel droplet size and velocity. The higher the pressure difference, the smaller are the droplet size distributions and the higher are the velocity distributions. Due to the presence of a very large number of droplets emerging from the dense spray, these droplets, while moving away from the injector, undergo collisions, coalescence, and energy exchange processes. Coalescence here indicates [Fig. 5(b)] that droplets collide due to relatively large velocity differences, and then coalesce into bigger droplets. Poon *et al.*[36] reported that the shape and deformation of the droplet is dependent not only on the size of the vortex ring, but also upon the free stream dynamic pressure and droplet pressure.

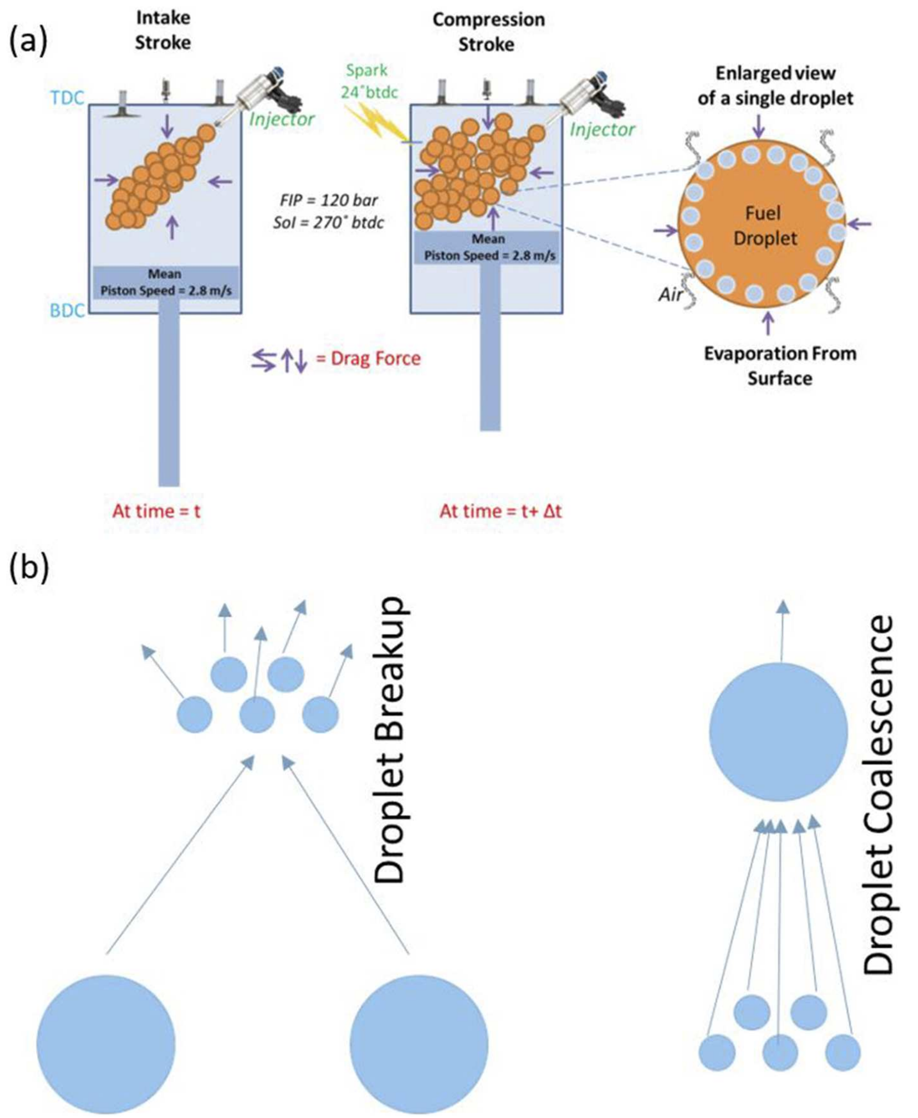

FIG. 5. (a) Schematic depicting evaporation from the periphery of the spray droplet in high-temperature and high-pressure environment in the combustion chamber. (b) Schematic illustrating droplet breakup and coalescence.

While traveling through the hot, high pressure combustion chamber environment, a fuel droplet would first be heated and expand, and then evaporate. Higher velocity of the droplets would lead them to undergo enhanced convection with faster evaporation, which initiates from the droplet boundary. This would be followed by mixing of fuel vapor with air and then the mixture formed will start burning after the spark initiation.

Life of a droplet in the combustion chamber mainly depends upon its size, mass, and velocity. The increased temperature of the combustion chamber and higher FIP results in the increased number of droplets with smaller size. As the droplet evaporation rate increases, SMD of the spray droplets increases (smaller droplets vanish first) and then decreases.[37] As the distance of a droplet from the injector increases, the evaporation rate increases, resulting in continuous reduction in the droplet size. A smaller droplet travelling in the wake of another droplet, will be travelling faster, and will tend to merge with the previous droplet to form a bigger droplet. If a droplet strikes the cylinder wall, it may stick to the wall or split into multiple smaller droplets. Also, owing to higher injection pressure and a small cylinder diameter, the fuel spray might impinge on the piston cavity/wall before being fully vaporized.[38] After impingement on the piston cavity/wall, droplets may splash-off.[39] A detailed experimental investigation of interaction processes of small liquid droplets with hot walls can be referred to in the literature.[40] An increase in the number of droplets increases the overall droplet surface area available for heat exchange with the hot, high pressure ambient air, which leads to enhanced evaporation.

Moukalled and Darwish[41] reported that liquid droplet mixing and evaporation is highly depended on turbulence created due to high speed of the engine. The GDI test engine used in these experiments is a small engine with high speed, swirl, squish, and tumble features. Turbulent reactive flows with fuel droplets are often encountered in a GDI engine, which have a dominant effect on the spray droplets.[42] Apart from these characteristics, there is intense turbulence in the combustion chamber, leading to recirculatory motion of spray droplets within the combustion chamber.[38,39] An inadequate penetration of spray in the combustion chamber would cause an inhomogeneous distribution of the fuel-air mixture. Therefore, for optimal engine performance, the spray fundamentals need to be understood very well and matched with the size and geometry of the combustion chamber.

To investigate the large scale features for sprays such as the one discussed above, optical imaging techniques have been used for over a century and continue to be used by employing volume illumination,[43] back-lit illumination,[44,45] shadowgraphy and Schlieren imaging[46,47] techniques, and the use of digital cameras has made these methods more prominent and efficient over time.

Figure 6 shows shadowgraphy of a typical GDI spray obtained in this study. As depicted in the image, sharp boundaries exist in the immediate vicinity of injector. These sharp boundaries exist because of high FIP leading to injection of high concentrations of high velocity spray droplets, which dominate the ambient air. Thereafter, spray droplets start vaporizing after the spray breaks up. Once the spray droplets start vaporizing, the vapor phase leads to gaseous expansion and droplets start losing their momentum due to vaporization and energy exchange.[48] The vapor phase is pushed aside by the incoming spray droplets, leading to an increased vapor/spray cone angle. In Fig. 6, most fuel vapor was observed to be concentrated in the sides of the sprays during the early injection stage. Vaporization proceeded from the periphery of the plume and the degree of vaporization was dependent on the FIP. Higher FIP increases the speed of the needle opening, preventing the formation of larger droplets shortly after the start of injection. Moreover, spray edges seemed to be inhomogeneous and spray plumes were hardly distinguishable from each other. Voids due to air entrapment between the two consecutive plumes were observed. Sharp spray boundaries closer to the nozzle lost their sharpness due to vortex formation as a result of close interaction of spray plumes with the ambient air. The spray plumes and subsequent vapor kept penetrating, even after almost complete vaporization of spray droplets. In the final stages, the spray plumes underwent significant distortion starting from near-nozzle region up to the end. At this stage, spray droplets are more sensitive to higher aerodynamic interaction with the ambient air because they are not surrounded closely by other spray jets. This spray behavior is largely attributed to kinematic viscosity and surface tension of the test fuel.

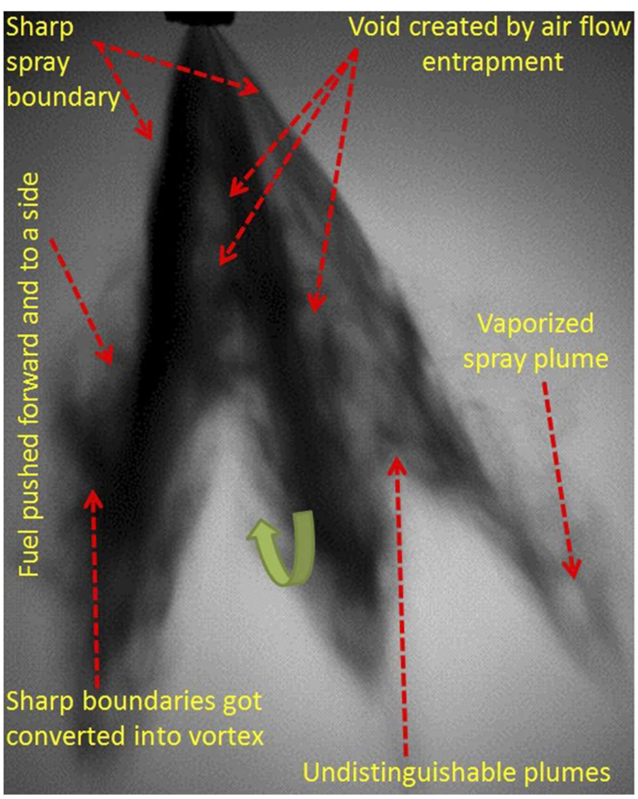

FIG. 6. Shadowgraphy of the gasoline direct injection spray plume.

Figure 7(a) shows the variation of exhaust gas temperature (EGT) with indicated mean effective pressure (IMEP) for the GDI test engine. EGT is a qualitative measure of bulk in-cylinder temperature, which directly affects pollutant formation. Relatively higher fuel quantity injected at a high engine load leads to higher bulk in-cylinder temperature. Relatively faster fuel-air charge motion at high engine speed leads to faster fuel-air mixing, which leads to relatively more complete combustion. The area of interest in this figure is highlighted, which corresponds to IMEP of 4 bars, when the EGT was ~450 °C. Figure 7(b) shows the variation of in-cylinder pressure, heat release rate (HRR), and mean gas temperature with respect to crank angle degrees (CAD) at 4 bars IMEP. The peak in-cylinder pressure was ~18 bars. HRR was negative over a period of 2-3 CAD bTDC due to the cooling effect of spray droplets, which absorbed heat from the combustion chamber for spray droplet vaporization. Beyond this, a sudden rise in HRR was observed, which corresponds to premixed combustion. In the GDI engine, the entire charge burns in a premixed combustion phase. Mean gas temperature increased with increasing crank angle and reached a maxima at ~38/35° CA aTDC before starting to decrease. It can be concluded from this graph that the shaded region (18 bars in-cylinder pressure and ~1400 K peak temperature) offers the highest probability of evaporation of fuel droplets. Figure 7(c) shows the distillation curve of gasoline. The distillation curve gives a direct measure of the fuel volatility characteristics. The information from the distillation curve will be helpful in explaining the spray droplet size and droplet velocity distributions obtained under different engine operating conditions. It was observed that droplet evaporation began at ~38 °C and ended at ~190 °C. However, this graph can be of interest in measuring the droplet size and velocity under ambient conditions only. Inside an engine combustion chamber environment, since there is very high temperature and pressure, spray droplets may experience drag forces in addition to intense turbulence, which affects droplet evaporation, spray breakup, droplet coalescence, and energy exchange processes. Particulate emissions for this operating condition are given in the supplementary material.

A. Spray droplet velocity distribution

Spray droplet velocity distribution variation can be divided into several subsections. These subsections include: injection delay,

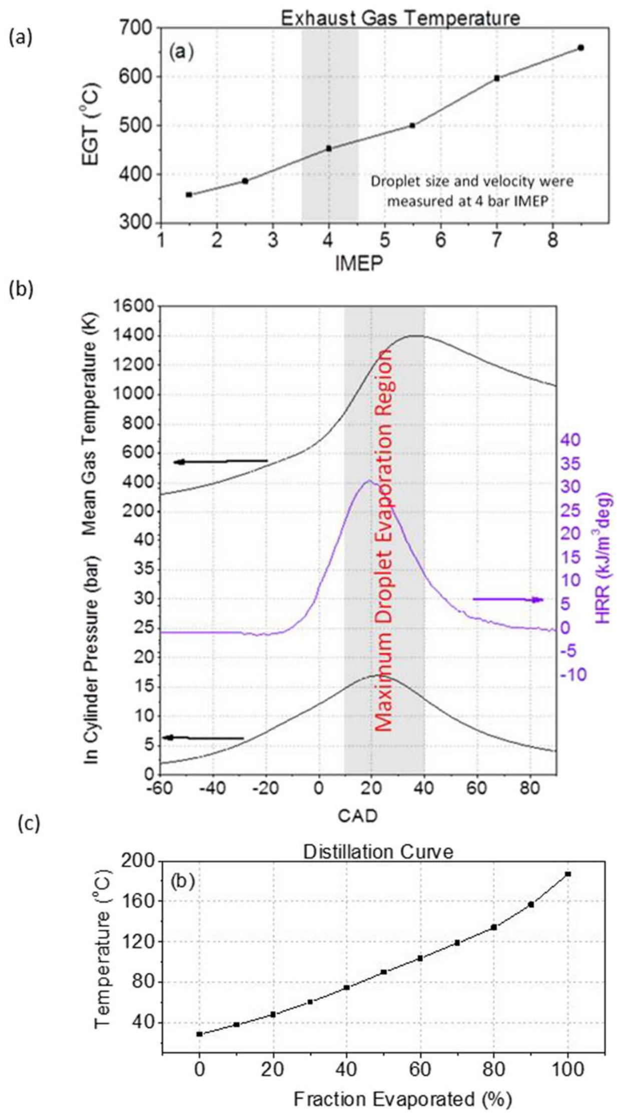

FIG. 7. (a) Variation of exhaust gas temperature as a function of IMEP. (b) Variation of in-cylinder pressure, HRR, and mean gas temperature with respect to CAD. (c) Distillation curve for gasoline.

detection time, and head and tail sections. Injection delay is the time difference between the start of energizing the injector solenoid and the start of actual injection. Detection time is the time interval between the start of injection and initial velocity signal of the spray droplets detected by the PDI system. Head section is the zone after the signal detection, where fuel droplets arrive as an ensemble in a region. This region has droplets with significant velocity. The point where droplet velocity tends to decrease (not constant) is considered as the end of the head section and the beginning of the tail section. Tail section is the zone where velocity is relatively lower and remains nearly constant with time.

Smaller, fast vaporizing droplets and good air entrainment into the spray are some of the essential requirements for the fuel sprays for engine applications. On the other hand, large, slow moving spray droplets and liquid fuel coming in contact with the cylinder walls is not at all desirable for the engine applications.

Figure 8 shows the droplet velocity component in the X-direction (V_x) for 10 ms pulse time and multiple injections under ambient conditions in the atmosphere and compared the same with V_x in the engine combustion chamber environment. Gasoline was the test fuel in both cases and an identical FIP of 120 bars was maintained. Each dot in the graph represents an individual spray droplet passing through the probe volume. The maximum value of V_x in the engine combustion chamber was 29.8 m/s, whereas in the CVSC under ambient conditions, the maximum value of V_x was 78.41 m/s, which was significantly higher than that in a firing engine, highlighting the importance of doing actual measurements in the engine combustion chamber. Similar results of high droplet velocity under atmospheric condition were reported by Lui *et al.*[49] and Li and Gebert.[50] This trend was attributed to the surface tension of the fuel droplets in the engine combustion chamber since surface tension significantly affects spray droplet formation, and eventually a large drag is experienced by the droplets in the engine combustion chamber, which has dynamic in-cylinder pressure and temperature conditions. This can be understood by the fact that the first droplets emerging from the nozzle are rapidly slowed down by the ambient air due to extreme drag and then they evaporate. Larger droplets have much higher inertia and higher fuel mass to surface area ratio; hence, their evaporation rate is rather slower.

As the spray droplets travel in the hot, high pressure environment of the engine combustion chamber, they heat up and partially evaporate. This reduces the surface tension of spray droplets as well as their size and velocity. In addition, spray droplets easily deform

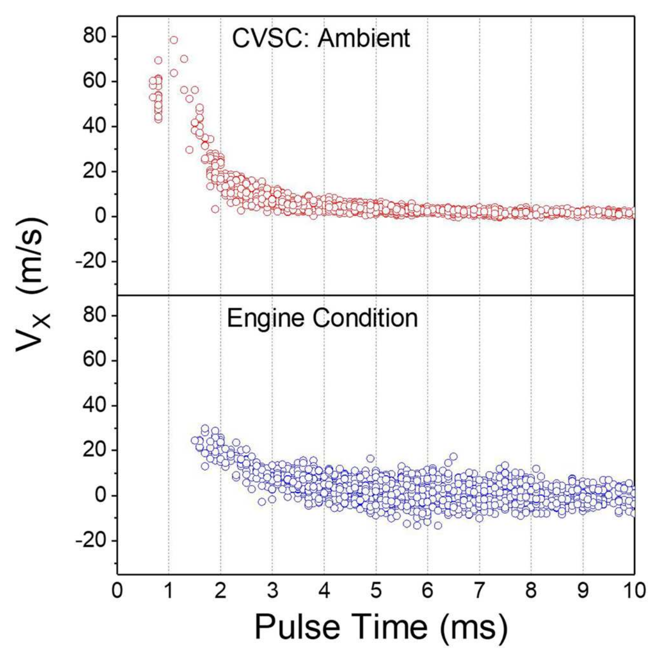

FIG. 8. Variations of droplet velocity V_x with pulse time in CVSC under ambient conditions with respect to the engine combustion chamber environment.

due to the aerodynamic drag they experience in the engine combustion chamber, leading to reduction in droplet velocity. The droplet size also reduces with increasing evaporation rate. In an engine's turbulent environment, droplets move randomly and eventually disintegrate in all directions. In an engine combustion chamber, smaller droplets move with the surrounding gas more readily with higher velocity compared to relatively larger droplets, which respond more slowly even with increased drag forces. The shape of larger droplets may distort under prevailing aerodynamic drag forces and higher slip velocities inside the engine combustion chamber. Therefore, large number of spray droplets vaporize prior to their detection in the head section, inside the engine combustion chamber. In addition to the in-cylinder temperature and pressure, the spray droplet vaporization rate also depends on the droplet diameter, droplet velocity, and fuel volatility. This is also the reason for nonexistence of the head section in the velocity-pulse time curve in the engine environment. A joint probability distribution function (PDF) depicting density of droplets along with droplet size distribution is given in the supplementary material.

Magnitudes of maximum negative velocity (−X direction) were 13.34 m/s in the engine combustion chamber and 0.88 m/s in the ambient atmosphere in CVSC. A relatively higher negative velocity of spray droplets in the engine environment was due to tumble air motion in the GDI engine combustion chamber, which forces the droplets to follow a tumbling airflow path in the direction of the piston motion and opposite to it. These negative velocity components are desirable because they enhance fuel-air mixing in the engine combustion chamber and therefore have a positive impact on the engine performance.

Normally, spray droplets at the edge of the spray plume are in direct contact with hot, high pressure turbulent air present in the engine combustion chamber. This turbulent airflow in the engine combustion chamber tends to separate smaller droplets from the large droplets and separates them into different trajectories due to inertial or air motion (swirl and tumble) effects. Larger spray droplets remain on the same path, whereas smaller spray droplets change their trajectory and vaporize rather quickly due to rapid heat and mass transfer with combustion chamber air at higher pressure and temperature. Larger droplets, which initially have a higher velocity and lower concentration, do not collide or coalesce with smaller droplets at a significant rate. Likewise, smaller droplets evaporate before much coalescence takes place. Such conditions obtained in the combustion chamber reduce droplet velocity distribution, as seen in Figs. 7 and 8.

Figure 9 shows the ensemble average of the droplet velocity component V_y for 10 ms pulse time acquired over multiple injections. Maximum V_y under engine conditions was 14.2 m/s and in CVSC under ambient conditions, it was 23.92 m/s. The magnitude of the maximum negative velocity component ($-V_y$) was 20.35 m/s under the engine conditions and 10.91 m/s under the ambient conditions, reflecting the effect of turbulence.

Figure 9 shows relatively lower variations in the velocity component V_y as compared to V_x (as shown in Fig. 8). As already discussed, the negative velocity component enhances fuel-air mixing and hence, improves the engine combustion. Like V_x, no head section was visible in V_y curves as well in both cases, which indicated that fuel droplets vaporized prior to the development of the head section in the droplet velocity-pulse time curve. These trends observed in droplet velocity components in the Y-direction were quite like those observed in the X-direction as well, the only difference being relatively lower average velocity magnitude in the previous case. A joint PDF depicting the density of droplets along with the droplet size distribution is given in the supplementary material.

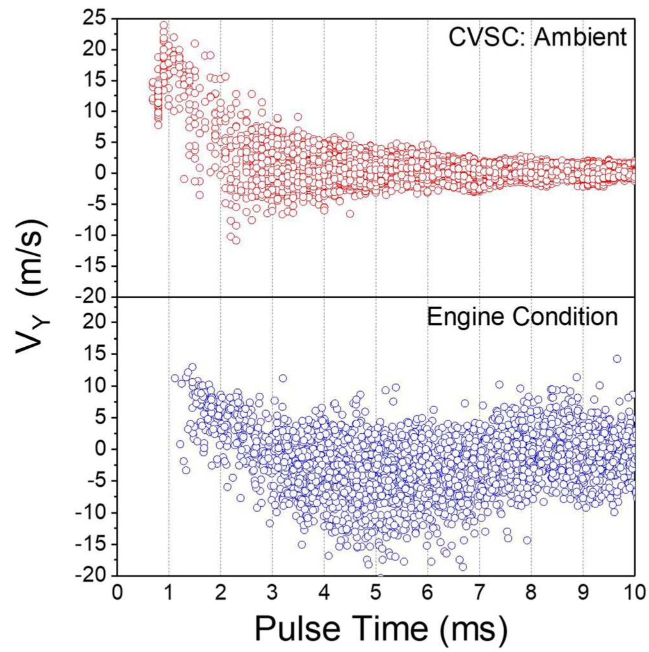

FIG. 9. Variations of the droplet velocity V_y with pulse time in CVSC under ambient conditions with respect to the engine combustion chamber environment.

B. Spray droplet size-velocity distribution

Figure 10 shows the comparative results of velocity component V_x in the engine combustion chamber environment and in CVSC under ambient conditions at an identical FIP of 120 bars. It can be seen from Fig. 10 that velocity under ambient conditions was significantly higher in CVSC than in the engine combustion chamber. Inside the engine, the bulk of spray droplets were concentrated near the origin and were relatively less scattered. PDI can measure reliably down to about 0.5 μm drop diameter. The range of droplet diameters in the CVSC under ambient conditions was from 0.5 to 75 μm and inside the engine combustion chamber, it ranged from 0.5 to 68 μm. However, the majority of spray droplets were found to be less than 28 μm diameter in both cases. The droplet size distribution in a spray depends on a complex chaotic combination of individual droplet breakup, coalescence, and evaporation inside the combustion chamber. Droplet breakup here means [Fig. 5(b)] spray droplets break-up into smaller ones due to their interaction with ambient air. These droplets interact with air moving at moderate velocity, hence experience drag force, leading to their break-up into smaller ones, as seen in the results above.

Since the fuel is injected into the cylinder, it may impact on liner wall or the piston cavity, leading to different possible interactions. These fuel droplets may eventually rebound or can possibly

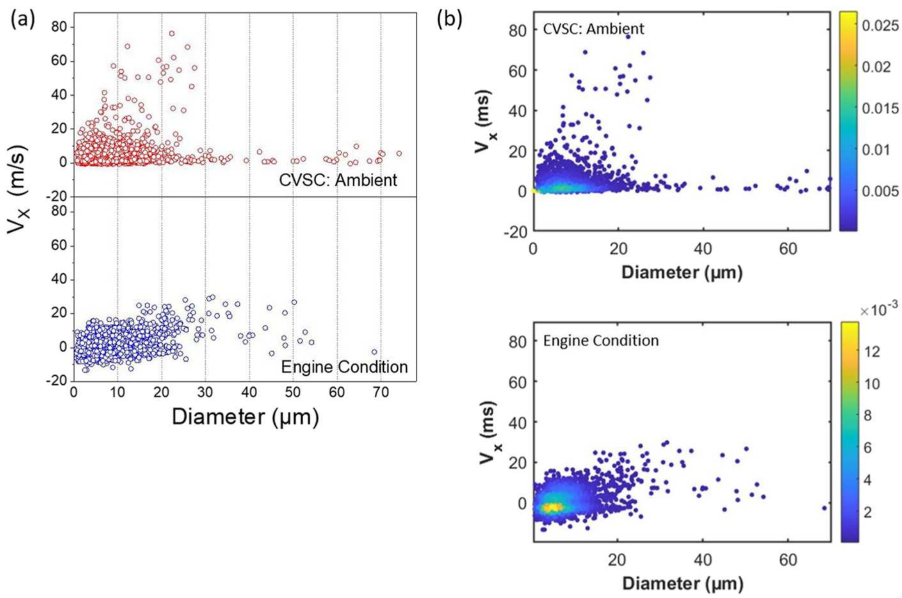

FIG. 10. (a) Variations in droplet velocity (V_x) with respect to the droplet diameter in the CVSC under ambient conditions and in the engine combustion chamber environment. (b) Joint PDF depicting the density of droplets from low to high along with droplet size distribution: Variations in droplet velocity (V_x) with respect to the droplet diameter in the CVSC under ambient conditions and in the engine combustion chamber environment.

stick to the piston or liner surface, or it may breakup and disperse in multiple directions. This in-turn depends on surface characteristics and kinetic energy of droplets at the time of impact. Smaller droplets bounce when they hit hot obstacles and do not burst. These smaller droplets do not contribute significantly to the piston wetting. On the other hand, a larger droplet may burst into smaller fuel droplets under the influence of drag forces and contribute significantly to piston wetting. This also suggests that slower evaporating droplets have higher mass, size and momentum. Present measurements in CVSC were made at a location slightly downstream of the spray breakup region, where the turbulence enhanced spray breakup is significant. Since the velocity and size of spray droplets were measured at a distance from the breakup region, the drag force exerted on the droplets during this interval was not significant. This is another reason for higher droplet size distribution under CVSC conditions.

The larger the velocity of droplets, the higher would be the drag force experienced by them. Therefore, droplets lose their mass and momentum quicker inside the engine combustion chamber environment (high pressure and temperature) than in the CVSC under ambient conditions, leading to relatively smaller droplet size distribution in the engine. Larger droplets in the CVSC under ambient conditions could be due to faulty measurements because of trajectory errors. However, larger droplets were not observed in the engine combustion chamber due to the high pressure and temperature environment. The reciprocating motion of the piston heats up the intake air and increases the evaporation rate of fuel spray droplets, resulting in smaller droplets inside the engine as seen in Fig. 10.

Figure 11(a) shows a comparison of the velocity component V_x with the pulse time in the CVSC under ambient conditions with that of the engine combustion chamber conditions. Initially, the average velocity V_x was significantly higher in the CVSC than that in the engine combustion chamber. Thereafter, average velocity V_x remained unchanged until after the end of the fuel injection. The high head section in the CVSC under ambient condition resulted in higher average droplet velocity as seen in Fig. 11(a). Similar values of velocity were reported in the literature by Badawy *et al.*,[51] and Yamaguchi *et al.*[52] for experiments conducted under ambient conditions in a CVSC.

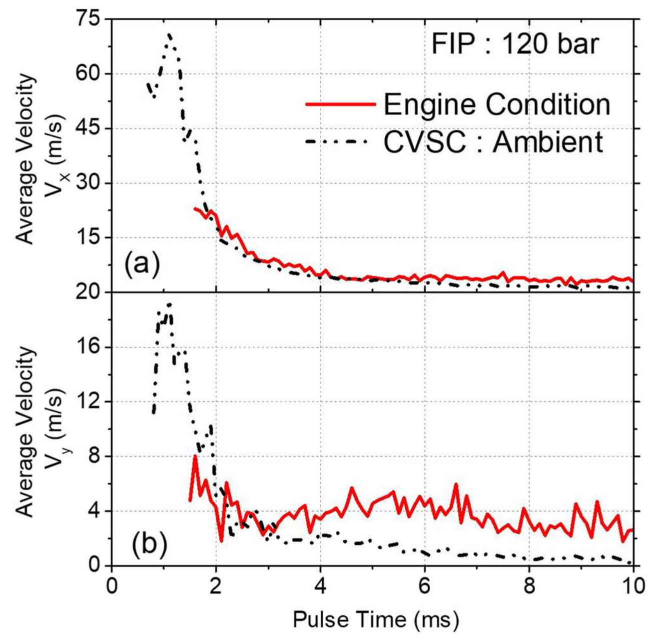

FIG. 11. Comparison of average velocity components (a) V_x and (b) V_y in CVSC under ambient conditions with average velocity components V_x and V_y under the engine combustion chamber conditions.

Figure 11(b) shows the comparison of the velocity component V_y with pulse time in CVSC under ambient conditions with that of the engine combustion chamber conditions. Initially, the average droplet velocity (V_y) was relatively higher in the CVSC than that in the engine combustion chamber conditions. Average droplet velocity (V_y) remained unchanged until after the end of the fuel injection in both cases. The higher head section under ambient conditions resulted in higher average droplet velocity. The average of V_y was identical for all engine load conditions.

SMD is widely accepted as an average droplet size parameter, and is widely used in mass transfer, and combustion calculations that controls the evaporation rate.[53] SMD is the mean of the ratio of droplet volume to droplet surface area for many droplets of a given fuel spray. In highly evaporative environment, SMD can increase initially due to evaporation and disappearance of the smaller droplets in the distribution. The droplet size controls the evaporation rate, mixing of air and fuel, and eventually pollutant formation. Figure 12 shows the comparison of SMD in the engine combustion chamber conditions and in the CVSC under ambient conditions. Due to time-resolved measurements with the PDI instrument and high data acquisition rates, mean values could be calculated with high accuracy. Relatively higher SMD for ambient conditions is attributed to relatively higher fuel viscosity and surface tension of gasoline (at lower temperature) under ambient conditions compared to engine combustion chamber conditions. Viscosity, surface tension, and latent heat of vaporization of fuel droplets decrease with increasing temperature, which sufficiently improves fuel injection and mixing processes.[54] These properties affect spray breakup therefore relatively larger droplets form under ambient conditions than those formed in the engine combustion chamber conditions. Average SMD was detected to be in the range of 4–8 μm under the engine combustion chamber conditions in the range of 11–15 μm in the CVSC under ambient conditions. Similar trends in results were reported in the literature by Jiang *et al.*,[55] Badawy *et al.*,[51] Yamaguchi *et al.*,[52] and Liu *et al.*[49] under ambient conditions (CVSC). Kim *et al.*[56] reported SMD (D_{32}) of 114.7 μm, 106.4 μm, and 99.4 μm for 30 mm, 50 mm, and 75 mm downstream of the nozzle tip and data were collected for a total of 10 000 droplets at 1 atm chamber pressure. Li and Gebert[50] reported similar trends in the SMD.[56,58] Under engine conditions, SMD was initially somewhat higher, which reduced gradually. On the other hand, under ambient conditions, SMD was initially 11 μm, which increased to 15 μm at a later stage. Another point to be noted was the difference in variation of the R^2 value of the curve fittings used for the engine combustion chamber and CVSC data as shown in Fig. 12. This showed that the data obtained under the engine conditions followed a definite trend, whereas the data obtained under the CVSC ambient conditions was rather scattered. This was mainly because the data acquired in the CVSC condition were obtained at a certain downstream distance and a given FIP, whereas under the engine combustion chamber conditions, various phenomena such as dynamic pressure change due to piston motion, turbulence, drag forces, and momentum exchange affected the spray pattern throughout the combustion chamber simultaneously. Subsequent injections are unlikely to interact with liquid fuel droplets from the first injection in the engine conditions because fuel spray droplet vaporization and combustion reactions occur very quickly in the engine unlike CVSC.[57] The data pertaining to the engine were for a constant engine speed, which created almost identical turbulence in the engine combustion chamber during successive engine cycles. Under ambient conditions in the CVSC, data were somewhat orderly up to 5 ms. This might be related to the injection duration, which was a few milliseconds inside the CVSC, and hence the pressure and velocity dominated the environment for only a short duration. It was the ambient conditions which started dominating later and affected the SMD of the spray droplets. As seen in the figure, the measurements in the CVSC were not so reliable at a larger pulse time due to the position of the probe volume.

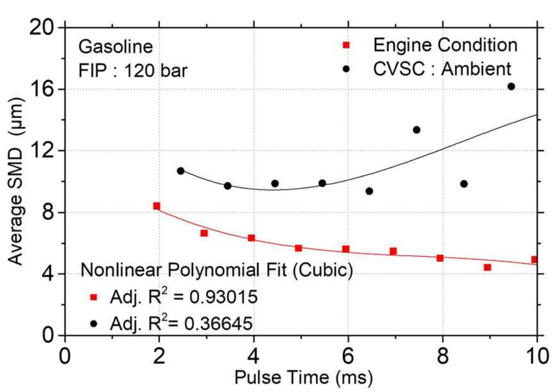

FIG. 12. Comparison of SMD with pulse time in the CVSC under ambient conditions and under the engine combustion chamber conditions.

C. Mean droplet size measurements

The life span of the fuel spray droplets is dependent on the rate of vaporization and combustion. Therefore, the knowledge of spatial distribution of droplets is important. Figure 13 shows the comparison of various mean droplet diameters in the engine combustion chamber environment and in the CVSC under ambient conditions.

Application of various mean droplet diameters is given in Table IV. It can be seen from Fig. 13 that under the engine

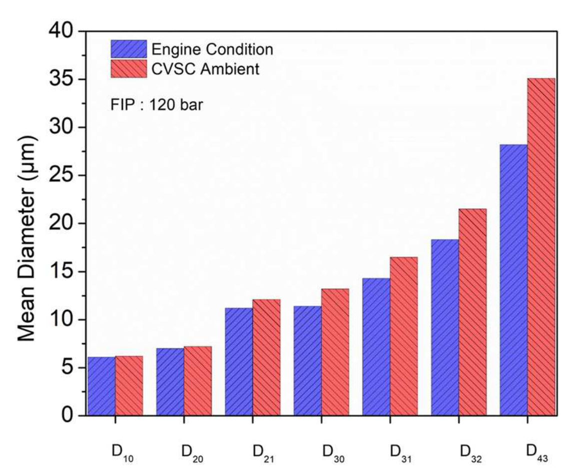

FIG. 13. Comparison of mean diameters in the engine combustion chamber conditions and in the CVSC under ambient conditions.

TABLE IV. Mean droplet diameters and their respective potential applications.[58,59]

Symbol	Common name of diameters	Definition	Application
D_{10}	Arithmetic mean (length)	$\frac{\sum N_i D_i}{\sum N_i}$	Comparison
D_{20}	Surface mean (surface area)	$\left[\frac{\sum N_i D_i^2}{\sum N_i}\right]^{1/2}$	Surface area controlling
D_{21}	Length mean (surface area length)	$\frac{\sum N_i D_i^2}{\sum N_i D_i}$	Absorption
D_{30}	Volume mean (volume)	$\left[\frac{\sum N_i D_i^3}{\sum N_i}\right]^{1/3}$	Volume controlling (hydrology)
D_{31}	Length mean (volume length)	$\left[\frac{\sum N_i D_i^3}{\sum N_i}\right]^{1/2}$	Evaporation, molecular diffusion
D_{32}	Sauter mean (volume-surface)	$\frac{\sum N_i D_i^3}{\sum N_i D_i^2}$	Mass transfer reaction
D_{43}	Herdan mean (De Brouckere or Herdan) (weight)	$\frac{\sum N_i D_i^4}{\sum N_i D_i^3}$	Combustion equilibrium

combustion chamber conditions, all mean droplet diameters were relatively smaller than those obtained in the CVSC under ambient conditions. This difference in mean droplet diameters was relatively narrower for D_{10} and D_{20}, but was the maximum for D_{43}. High temperature and pressure environment in the engine combustion chamber at the end of compression stroke heats up the spray droplets to a great extent and leads to greatly enhanced evaporation compared with CVSC under ambient conditions, resulting in smaller mean diameters (depletion of a larger size droplet via evaporation due to high temperature and pressure).

As mentioned earlier, smaller spray droplets lose their momentum due to large drag from the circulating ambient air. This drag force of ambient air was significantly higher under the engine combustion chamber conditions compared to the CVSC under ambient conditions. That is why the mean diameter in the engine combustion chamber conditions was relatively lower than that inside the CVSC under ambient conditions. The droplet diameter under the engine combustion chamber conditions could be even smaller than those obtained from these experiments. There is a possibility of higher rate of spray droplets coalescence in the engine combustion chamber environment. Coalescence occurs in the secondary spray breakup zone. Smaller droplets combine with larger droplets because of the effect of drag forces. Hence, the droplet size should increase in the engine combustion chamber environment. However, individual spray droplet diameter in the engine environment was significantly smaller than the diameter measured in the CVSC under ambient conditions.

Kinematic viscosity of the test fuel was the most influential factor amongst several others and could be responsible for this trend of mean diameter as observed in Fig. 13. Fuel spray droplets experienced a significantly higher temperature environment in the engine combustion chamber prior to their evaporation and eventually combustion, which also reduced fuel viscosity, followed by the reduction in diameters of the spray droplets. Increased temperature in the engine combustion chamber also reduced the surface tension of the fuel spray droplets, leading to further reduction in the droplet size distribution too.

Significantly higher fuel spray atomization may cause some negative impact on the combustion. Finer spray droplets may not be able to cross the entire combustion chamber since they evaporate relatively earlier than larger droplets and thus, the fuel vapors may remain concentrated in specific combustion chamber zones, forming fuel rich zones, thus adversely impacting the combustion possibly. Therefore, FIP should be optimized for combustion stability, efficiency, and emissions in GDI engines.

The PDI instrument measures the droplet size, velocity, and time of arrival of each droplet transiting the measurement volume. These results are saved in each data file and can be used for higher level droplet dynamics analysis. For observation, the size measurements are sorted into bins and counts to produce a histogram of the size and of the velocity (PDF's). For these PDFs, the bin resolution can be adjusted to meet the requirements of the observations. The PDFs provide a ready observation of the droplet size distributions at each location within the spray chamber or engine. At the same time, the various mean values for the drop size (D_{10}, D_{20}, D_{32}, and D_{30}) are calculated. For the velocity measurements, the mean velocity and the drop velocity fluctuation information are provided based on the actual measurements, not on the bin PDF results. Direct measurements of the velocity size distributions are informative for researchers making observations on the relative populations of different size classes. One must understand that the various sized droplets serve to convey the fuel into the combustion chamber with the small sized droplets evaporating first and the larger sized droplets penetrating deeper into the combustion environment distributing the fuel to more distant locations. Combustion researchers require these size distributions in order to assess the effects of the droplet size distribution on the fuel-air mixing and reaction thermodynamics. Thus, the PDFs of droplet size and velocity are critical to the understanding of the spray dynamics and an essential part of the spray flow information. Figure 14 shows the probability distribution function (PDF) of the droplet diameter obtained in the CVSC under ambient conditions and under the engine combustion chamber conditions corresponding to Figs. 8–10. The corresponding drop diameter distribution is approximately Gaussian, like the one reported in

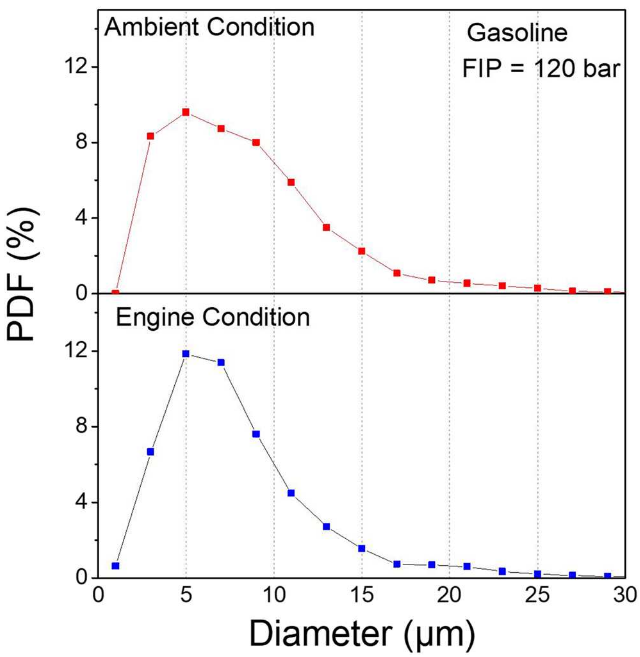

FIG. 14. Variations in PDF with droplet diameter in the CVSC under ambient conditions and in the engine combustion chamber environment.

the literature.[10] A range of diameters from 1 to 30 μm were found in both engine and CVSC. Though the probability of finding 5 μm diameter droplets was higher in both the engine and CVSC conditions, PDF (%) was relatively higher in the engine. Similar trends in results were reported in the literature by Jiang *et al.*[55] and Pei *et al.*[60] albiet under ambient conditions in the CVSC. For the same mass of the fuel injected, spray atomization with finer droplets was achieved under engine conditions, which resulted in superior fuel-air mixing compared to the CVSC under ambient conditions. Due to relatively higher difference in spray droplet velocities and ambient air in the engine environment, greater drag forces were experienced by spray droplets, which could lead to an unstable growth of waves on the droplet surface, which eventually led to disintegration of spray droplets further and formed new, smaller droplets. These finer droplet sizes and therefore a larger specific surface area of evaporating smaller droplets highly intensify the mass transfer, and therefore the formation of combustible mixture in the gaseous phase.[61]

VII. CONCLUSIONS

Real time measurements and comparative analysis of the droplet size and velocity distributions in a GDI optical engine combustion chamber and a CVSC were performed successfully in this study for the first time. It was found that the fuel-air mixing and droplet size-velocity distribution measurements in the engine combustion chamber were affected by the test fuel properties, such as fuel density, viscosity, and surface tension, and by the mixing rate of the fuel and intake air, which changed with inlet air temperature and pressure. There existed sharp spray boundaries just beneath the injector since high FIP was dominant in an ambient environment in a CVSC. The edges seemed to become "evenly inhomogeneous" and the individual spray plumes were hardly distinguishable. Maximum spray droplet velocity components (V_x, V_y) in the engine combustion chamber conditions were 29.8 m/s, 14.2 m/s and in the CVSC under ambient conditions, they were 78.41 m/s, 23.92 m/s, respectively, showing a large difference between the two conditions. In the engine combustion chamber environment, the bulk of spray droplets were concentrated near the origin of graph (0–10 μm) and were observed to be less scattered. The average SMD of the spray droplets was always found to be smaller in the case of the engine combustion chamber conditions compared to the CVSC under ambient conditions. The probability of existence of smaller micrometer-sized droplets was relatively higher under the engine combustion chamber conditions, but these droplets disappear rapidly due to evaporation.

Engine fuel spray measurements *ex situ* are useful but provide limited information on the actual engine conditions which includes highly transient and turbulent reacting flow effects. Quiescent conditions in the combustion chamber simulations provide limited information and, in some cases, can lead to misleading observations when addressing transient flows with reaction. These *in situ* data provide a significant advancement toward a better understanding of in-cylinder transient reacting conditions. The findings of this study will be very useful for upgrading the existing knowledge in the field of fuel-air mixture preparation in the engine combustion chamber and updating the database for scientists involved in developing CFD codes and their validation using these real engine spray velocity and size distribution data.

VIII. OPEN QUESTIONS/ SCOPE OF FUTURE WORK

The objective of this experimental investigation was that such measurements are possible, can provide useful data, and reveal differences between the two environments. Another objective of this experimental campaign was to develop a methodology to measure the droplet size and velocity distributions inside a firing optical engine. There are a few open questions and future scope of work:

- Fuel: Standard gasoline with no oxygenate was used in this experimental investigation. Fuel companies are continuously developing new and renewable fuels to meet stringent emission norms. The investigation can benefit fuel refineries, and therefore, can be extended to oxygenated fuels to know the spray droplet-size distribution so that combustion can be made efficient and emissions can be reduced.
- Fuel Injection pressure: Injectors for GDI engines are being designed to deliver higher fuel injection pressure. Higher fuel injection pressure may lead to even smaller droplet size distribution and relatively more homogeneous fuel air mixture.
- Different locations for measurement in the combustion chamber: This experimental investigation measures the droplet size distribution at the center of the optical window in one plane. It is extremely challenging to make measurements at different locations due to the curvature of the optical window, access of laser beams to pass through the optical liner, while maintaining the focal length and injector position.

- Three-dimensional velocity: In this paper, two components of velocity were measured due to the limitation of access of laser beam to pass through the optical window.
- Compression ignition engine: It is difficult to measure the droplet size distribution in a compression ignition engine because fuel is injected in the compression stroke in the piston cavity, where there is hardly any optical access possible at TDC location. In addition, the time window available to measure the droplet size is rather small. However, the effects of multiple injection strategies (first injection in the intake and last injection in the exhaust stroke) may possibly be investigated.
- Advanced engine techniques: PDI can be used to measure and optimize combustion in HCCI/PCCI/RCCI engine technologies by measuring droplet velocity and size distribution.

SUPPLEMENTARY MATERIAL

The supplementary material includes sections on quantification of the associated uncertainties and validation, procedure of laser beam alignment, assessment of spray droplet velocity distribution, particulate emission, and safety.

ACKNOWLEDGMENTS

The authors would like to acknowledge the research grant received from Committee for the Acquisition of Research Equipment (CARE), and the Indian Institute of Technology Kanpur, Kanpur, India for procurement of the PDI instrument. The authors would also like to thank Mr. Mike Houser from Artium technologies, Sunnyvale, California, for his assistance in the initial experiments.

REFERENCES

[1] W. Bachalo, C. Hess, and C. Hartwell, "An instrument for spray droplet size and velocity measurements," J. Eng. Power **102**, 798 (1980).

[2] M. Nakamura, F. Akamatsu, R. Kurose, and M. Katsuki, "Combustion mechanism of liquid fuel spray in a gaseous flame," Phys. Fluids **17**, 123301 (2005).

[3] A. Moosavian, G. Najafi, B. Ghobadian, and M. Mirsalim, "The effect of piston scratching fault on the vibration behavior of an IC engine," Appl. Acoust. **126**, 91 (2017).

[4] K. S. Varde and D. M. Popa, "Diesel fuel spray penetration at high injection pressures," in SAE Technical Paper No. 830448, 1983.

[5] Y. Pan and K. Suga, "Numerical simulation of binary liquid droplet collision," Phys. Fluids **17**, 082105 (2005).

[6] T. Hori, J. Senda, T. Kuge, and H. Fujimoto, "Large eddy simulation of non-evaporative and evaporative diesel spray in constant volume vessel by use of KIVALES," in SAE Technical Paper No. 2006-01-3334, 2006.

[7] Y. Yi and C. M. DeMinco, "Numerical investigation of mixture preparation in a GDI engine," in SAE Technical Paper No. 2006-01-3375, 2006.

[8] T. Su, C. Chang, R. D. Reitz, P. Farrell, A. Pierpont, and T. Tow, "Effects of injection pressure and nozzle geometry on spray SMD and D.I. emissions," SAE Technical Paper No. 952360, 1995.

[9] M. Schmitt, C. Frouzakis, Y. Wright, A. Tomboulides, and K. Boulouchos, "Investigation of cycle-to-cycle variations in an engine-like geometry," Phys. Fluids **26**, 125104 (2014).

[10] W. Bachalo and M. Houser, "Spray drop size and velocity measurements using the phase/Doppler particle analyzer," Int. J. Turbo Jet Engines **4**, 207 (1987).

[11] K. N. Premnath and J. Abraham, "Simulations of binary drop collisions with a multiple-relaxation-time lattice-Boltzmann model," Phys. Fluids **17**, 122105 (2005).

[12] M. Y. Naz, S. A. Sulaiman, and B. Ariwahjoedi, "Spatio-temporal droplet size statistics in developing spray of starchy solution," AIP Conf. Proc. **1669**, 020033 (2015).

[13] F. Augier, O. Masbernat, and P. Guiraud, "Slip velocity and drag law in a liquid-liquid homogeneous dispersed flow," AIChE J. **49**, 2300 (2003).

[14] T.-W. Lee and K. An, "Quadratic formula for determining the drop size in pressure-atomized sprays with and without swirl," Phys. Fluids **28**(6), 063302 (2016).

[15] C. McCreath and J. Beer, "A review of drop size measurement in fuel sprays," Appl. Energy **2**, 3 (1976).

[16] A. Jones, "A review of drop size measurement—The application of techniques to dense fuel sprays," Prog. Energy Combust. Sci. **3**, 19 (1977).

[17] N. A. Chigier, *The Atomization and Burning of Liquid Fuel Sprays* (Elsevier, 1979).

[18] B. Vukasinovic, M. K. Smith, and A. Glezer, "Spray characterization during vibration-induced drop atomization," Phys. Fluids **16**, 306 (2004).

[19] W. D. Bachalo, "Method for measuring the size and velocity of spheres by dual-beam light-scatter interferometry," Appl. Opt. **19**, 363 (1980).

[20] W. Bachalo, "Spray diagnostics for the twenty-first century," Atomization Sprays **10**, 439 (2000).

[21] C. Tropea, "Optical particle characterization in flows," Annu. Rev. Fluid Mech. **43**, 399 (2011).

[22] M. Yamakawa, S. Isshiki, J. Lee, and K. Nishida, "3-D PIV analysis of structural behavior of D.I. gasoline spray," SAT Technical Paper No. 2001-01-3669, 2001.

[23] S. Lee and S. Park, "Experimental study on spray break-up and atomization processes from GDI injector using high injection pressure up to 30 MPa," Int. J. Heat Fluid Flow **45**, 14 (2014).

[24] S. H. Park, H. J. Kim, H. K. Suh, and C. S. Lee, "Atomization and spray characteristics of bioethanol and bioethanol blended gasoline fuel injected through a direct injection gasoline injector," Int. J. Heat Fluid Flow **30**, 1183 (2009).

[25] T. Anand, A. M. Mohan, and R. Ravikrishna, "Spray characterization of gasoline-ethanol blends from a multi-hole port fuel injector," Fuel **102**, 613 (2012).

[26] M. Heldmann, T. Knorsch, and M. Wensing, "Investigation of fuel atomization and evaporation of a DISI injector spray under homogeneous charge conditions," SAE Int. J. Engines **6**, 1213 (2013).

[27] Y. Huang, S. Huang, R. Huang, and G. Hong, "Spray and evaporation characteristics of ethanol and gasoline direct injection in non-evaporating, transition and flash-boiling conditions," Energy Convers. Manage. **108**, 68 (2016).

[28] P. Aleiferis, J. Serras-Pereira, Z. Van Romunde, J. Caine, and M. Wirth, "Mechanisms of spray formation and combustion from a multi-hole injector with E85 and gasoline," Combust. Flame **157**, 735 (2010).

[29] N. Sharma and A. K. Agarwal, "An experimental study of microscopic spray characteristics of a GDI injector using phase Doppler interferometry," in SAE Technical Paper No. 2016-28-0006, 2016.

[30] A. K. Agarwal, S. Gadekar, and A. P. Singh, "In-cylinder air-flow characteristics of different intake port geometries using tomographic PIV," Phys. Fluids **29**, 095104 (2017).

[31] A. Saha, J. D. Lee, S. Basu, and R. Kumar, "Breakup and coalescence characteristics of a hollow cone swirling spray," Phys. Fluids **24**, 124103 (2012).

[32] S. S. Yoon, "Droplet distributions at the liquid core of a turbulent spray," Phys. Fluids **17**, 035103 (2005).

[33] W. Bachalo, "Complete particle field characterization with optical diagnostics," J. Laser Appl. **1**, 33 (1989).

[34] S. V. Sankar, K. E. Maher, D. M. Robart, and W. D. Bachalo, "Rapid characterization of fuel atomizers using an optical patternator," J. Eng. Gas Turbines Power **121**, 409 (1999).

[35] Z.-F. Zhou, G.-Y. Lu, and B. Chen, "Numerical study on the spray and thermal characteristics of R404A flashing spray using OpenFOAM," Int. J. Heat Mass Transfer **117**, 1312 (2018).

[36] E. K. Poon, J. Lou, S. Quan, and A. S. Ooi, "Effects of streamwise rotation on the dynamics of a droplet," Phys. Fluids **24**, 082107 (2012).

[37] H. Guo, X. Ma, Y. Li, S. Liang, Z. Wang, H. Xu, and J. Wang, "Effect of flash boiling on microscopic and macroscopic spray characteristics in optical GDI engine," Fuel **190**, 79 (2017).
[38] Z. Si, N. Shimasaki, K. Nishida, Y. Ogata, M. Guo, C. Tang, and Z. Huang, "Experimental study on impingement spray and near-field spray characteristics under high-pressure cross-flow conditions," Fuel **218**, 12 (2018).
[39] H. Luo, K. Nishida, S. Uchitomi, Y. Ogata, W. Zhang, and T. Fujikawa, "Microscopic behavior of spray droplets under flat-wall impinging condition," Fuel **219**, 467 (2018).
[40] A. Karl and A. Frohn, "Experimental investigation of interaction processes between droplets and hot walls," Phys. Fluids **12**, 785 (2000).
[41] F. Moukalled and M. Darwish, "Mixing and evaporation of liquid droplets injected into an air stream flowing at all speeds," Phys. Fluids **20**, 040804 (2008).
[42] W. P. Jones, A. J. Marquis, and D. Noh, "An investigation of a turbulent spray flame using large eddy simulation with a stochastic breakup model," Combust. Flame **186**, 277 (2017).
[43] A. Marchi, J. Nouri, Y. Yan, and C. Arcoumanis, "Spray stability of outwards opening pintle injectors for stratified direct injection spark ignition engine operation," Int. J. Engine Res. **11**, 413 (2010).
[44] J. Manin, M. Bardi, and L. M. Picket, "Evaluation of the liquid length via diffused back-illumination imaging in vaporizing diesel sprays," in The Eighth International Conference on Modeling and Diagnostics for Advanced Engine Systems (COMODIA2012), Fukuoka, Japan, July 23–26, 2012.
[45] J. Ghandhi and D. Heim, "An optimized optical system for backlit imaging," Rev. Sci. Instrum. **80**, 056105 (2009).
[46] G. S. Settles, *Schlieren and Shadowgraph Techniques: Visualizing Phenomena in Transparent Media* (Springer Science & Business Media, 2012).
[47] T. D. Fansler and S. E. Parrish, "Spray measurement technology: A review," Meas. Sci. Technol. **26**, 012002 (2014).
[48] M. Pilch and C. Erdman, "Use of breakup time data and velocity history data to predict the maximum size of stable fragments for acceleration-induced breakup of a liquid drop," Int. J. Multiphase Flow **13**, 741 (1987).
[49] Y. Liu, Y. Pei, Z. Peng, J. Qin, Y. Zhang, Y. Ren, and M. Zhang, "Spray development and droplet characteristics of high temperature single-hole gasoline spray," Fuel **191**, 97 (2017).
[50] S.-C. Li and K. Gebert, "Spray characterization of high pressure gasoline fuel injectors with swirl and non-swirl nozzels," SAT Technical Paper No. 981935, 1998.
[51] T. Badawy, M. A. Attar, P. Hutchins, H. Xu, J. K. Venus, and R. Cracknell, "Investigation of injector coking effects on spray characteristic and engine performance in gasoline direct injection engines," Appl. Energy **220**, 375 (2018).
[52] A. Yamaguchi, L. Koopmans, A. Helmantel, F. P. Karrholm, and P. Dahlander, "Spray characterization of gasoline direct injection sprays under fuel injection pressures up to 150 MPa with different nozzle geometries," in SAE Technical Paper No. 2019-01-0063, 2019.
[53] A. H. Lefebvre and V. G. McDonell, *Atomization and Sprays* (CRC Press, 2017).
[54] P. G. Drazin and W. H. Reid, *Hydrodynamic Stability* (Cambridge University Press, 2004).
[55] C. Jiang, H. Xu, D. Srivastava, X. Ma, K. Dearn, R. Cracknell, and J. Krueger-Venus, "Effect of fuel injector deposit on spray characteristics, gaseous emissions and particulate matter in a gasoline direct injection engine," Appl. Energy **203**, 390 (2017).
[56] H. Kim, S. Tongchai, and O. Lim, "A study on the particle size and velocity profile on a gasoline port injector using a phase Doppler particle analyzers (PDPA)," Energy Procedia **145**, 374 (2018).
[57] B. W. Knox and C. L. Genzale, "Scaling combustion recession after end of injection in diesel sprays," Combust. Flame **177**, 24 (2017).
[58] R. Mugele and H. Evans, "Droplet size distribution in sprays," Ind. Eng. Chem. **43**, 1317 (1951).
[59] H. Liu, *Science and Engineering of Droplets: Fundamentals and Applications* (William Andrew, 1999).
[60] Y. Pei, J. Qin, X. Li, D. Zhang, K. Wang, and Y. Liu, "Experimental investigation on free and impingement spray fueled with methanol, ethanol, isooctane, TRF and gasoline," Fuel **208**, 174 (2017).
[61] M. A. Benmahammed, B. Veyssiere, B. A. Khasainov, and M. Mar, "Effect of gaseous oxidizer composition on the detonability of isooctane–air sprays," Combust. Flame **165**, 198 (2016).